Understanding the Mechanism of Superoxide Reductase Promoted Reduction of Superoxide

Lisa M. Brines[a] and Julie A. Kovacs*[a]

Superoxide reductases (SORs) are nonheme, iron-containing enzymes which reduce superoxide (O_2^-) to hydrogen peroxide (H_2O_2) in anaerobic organisms. In contrast to the classical superoxide dismutases (SODs), SORs selectively reduce, rather than disproportionate, superoxide at an unusual [Fe(NHis)$_4$SCys] catalytic site. Studies of the native enzyme and mutants have suggested the formation of a transient ferric-(hydro)peroxide intermediate in SOR's catalytic cycle, with subsequent protonation to yield hydrogen peroxide and a glutamate-bound ferric resting state. With the synthesis of small molecular model compounds of the enzyme's active site, analogous intermediates can be more thoroughly investigated in order to understand how the structure at the nonheme iron active site affects its function. Specific goals include the understanding of the role of the *trans* cysteinate in the promotion of SOR chemistry, as well as the role of the protons in the mechanism of the reaction. Because hydrogen peroxide formation requires two protons, investigation of the proton-dependence of the formation of ferric-(hydro)peroxo model complexes, as well as their subsequent reactivity with proton donors, yields important information about possible mechanisms. As new biochemical data on SORs become available, synthetic modeling, biophysical characterization, and DFT calculations continue to be important tools in the identification of viable mechanistic pathways.

(© Wiley-VCH Verlag GmbH & Co. KGaA, 69451 Weinheim, Germany, 2007)

1. Introduction

Organisms exposed to molecular oxygen inevitably encounter reactive oxygen species that are formed by the adventitious reduction of O_2 by redox-active enzymes.[1] These species include superoxide, O_2^-, the one-electron-reduced product of dioxygen. Elevated superoxide levels have been implicated in a number of diseases including diabetes[2] and the cell death and tissue damage that occurs following a stroke or heart attack.[3] Severe neurological disorders such as Parkinson's[4,5] and Alzheimer's[6,7] diseases may also be related to nerve cell damage caused by O_2^-. Additionally, some types of cancer are thought to arise from mutations induced by O_2^- damage to DNA.[8,9] Organisms have evolved two known defenses for the detoxification of superoxide. In particular, two classes of enzymes have been identified whose function is the reduction and/or oxidation of superoxide: the superoxide dismutases (SODs) and the superoxide reductases (SORs).[10–16] The classical SODs disproportionate superoxide to hydrogen peroxide and dioxygen. In contrast, SORs selectively reduce superoxide to hydrogen peroxide in anaerobic organisms without the formation of dioxygen as a byproduct. How SORs are able to selectively reduce O_2^- and avoid SOD activity is still not well understood. The active site's redox potential and access to protons are key parameters that govern this reactivity (vide infra).

[a] Department of Chemistry, University of Washington, Box 351700, Seattle, WA 98195, USA
Fax: +1-206-685-8665
E-mail: kovacs@chem.washington.edu

$$O_2^{\bullet-} + 2H^+ + e^- \xrightarrow{\text{SOR}} H_2O_2$$

$$2O_2^{\bullet-} + 2H^+ \xrightarrow{\text{SOD}} O_2 + H_2O_2$$
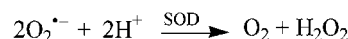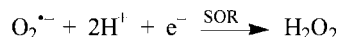
Julie Kovacs (left) received her Ph. D. from Harvard in 1986, and was a President's Postdoctoral Fellow at U. C. Berkeley from 1986–88. She has been on the faculty at the University of Washington, in Seattle, since 1988, where she is currently a full Professor of Chemistry. Her interest in metalloenzymes developed while at Harvard. Her research focuses on the synthesis of thiolate-ligated transition-metal complexes and on the comprehension of how sulfur ligands influence function in cysteinate-ligated nonheme iron enzymes.

Lisa M. Brines (right) was born in Spokane, Washington, USA. She received a Bachelor of Science degree in Chemistry from Seattle University in 2002 and later that year joined the Department of Chemistry at the University of Washington as a graduate student. She works in Professor Kovacs' group and studies the active sites of metalloenzymes with the use of synthetic modeling techniques.

In order to confirm the viability of the proposed intermediates in the mechanism of enzymatic superoxide reduction, synthetic models have proven useful in the establishment of spectroscopic parameters with which the biochemical data can be compared. Interpretation of the protein structure in relation to its function can be complicated by a lack of resolution of the spectra or the inability to trap intermediates because of solvent constraints. Small molecules are often used to trap and characterize key intermediates that may not be observable in the enzyme. In combination, biochemical and synthetic modeling data have begun to generate a clearer picture of the mechanism of superoxide reduction. These data include information on the role of the *trans* thiolate in the nonheme iron active site and the effect of spin-state on the reactivity of the proposed peroxobound ferric intermediates. Furthermore, exploration of the reactivity of synthetic peroxide intermediates with proton donors in a controlled fashion may help elucidate the identity and role of proton donors in the SOR-catalyzed reduction of O_2^- to H_2O_2.

2. Superoxide Reductases (SORs)

Five crystal structures of SOR have been reported from four different bacterial sources: *Pyrococcus furiosus*,[17] *Desulfovibrio desulfuricans*,[18] *Treponema palladium*,[19] and *Desulfoarculus baarsii*.[20] In the catalytically active reduced state, SORs contain a high-spin ($S = 2$) Fe^{II} center (center II) ligated by four equatorial histidine units and one apical cysteinate residue *trans* to an open site (Figure 1). Additionally, a number of SORs also contain a second rubredoxin-like [Fe(SCys)$_4$] center (center I) and are sometimes termed 2Fe-SORs to indicate the presence of a second iron site.[16] The C13S mutant of *D. vulgaris* 2Fe-SOR leads to the loss of center I, but does not prevent SOR activity.[21] Thus, center I is not believed to participate in the catalytic cycle. In the oxidized resting state, the active site is high-spin ($S = 5/2$) and contains a glutamate moiety coordinated to the sixth axial site. This glutamate (Glu^{14} or Glu^{47}, depending on the organism) is attached to a solvent-exposed flexible loop region of the protein and moves to a distance of 7.1 Å away from the metal ion upon reduction to the Fe^{II} state.[17] This flexible loop region also contains a conserved lysine (Lys^{47} or Lys^{48}) unit that has been proposed to play an essential role in the promotion of the catalytic activity of SOR by the attraction of the anionic superoxide ion to the enzyme's active site via coulombic forces.[22,23] The ammonium group of this lysine unit lies 6–12 Å away from the iron center. Because two protons are necessary to form H_2O_2, protonation of (Fe–η^2-O_2) or (Fe–η^1-OOH) intermediates plays an important role in the overall mechanism of superoxide reduction by SOR. The identity of the two proton sources is currently under investigation in the wild-type (WT) and mutant enzymes and through the study of synthetic enzyme active site models.
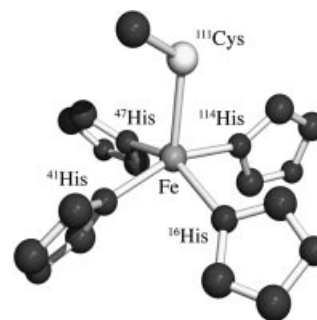

Figure 1. Active site of the reduced catalytically active form of the nonheme iron enzyme superoxide reductase (SOR).

2.1 SOD versus SOR

SODs disproportionate O_2^- into hydrogen peroxide and dioxgen in aerobic organisms.[13,14,24] In contrast, SORs selectively reduce O_2^- to hydrogen peroxide; this avoids the formation of dioxygen, which would otherwise be toxic to the anaerobic organisms that contain them.[10,12,25] Bacterial SODs typically contain either nonheme iron or manganese at the active site (FeSOD or MnSOD) although copper–zinc (Cu, ZnSOD) and nickel (NiSOD) enzymes are also known.[26,27] Reduced FeSODs contain a nonheme iron active site ligated by three histidine units, an aspartate group, and a H_2O/OH^- ligand (pK_a = 8.5) supported by a conserved H-bonding network. The azide-inhibited oxidized form has been crystallographically characterized and possesses the structure shown in Figure 2. A coordination environment with a 2His-1-carboxylate motif is common among nonheme iron enzymes.[28] In contrast, SOR is part of a new class of nonheme iron enzymes that contain a thiolate moiety in the coordination sphere.[29] Recent reviews describe the superoxide dismutase (SOD) mechanism and biophysical properties in more detail.[13,14,26]
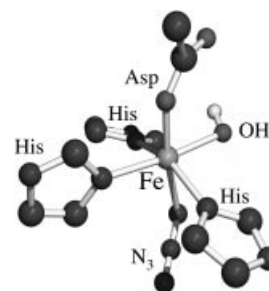

Figure 2. Active site of the oxidized azide-inhibited form of iron superoxide dismutase (Fe-SOD).

FeSODs and MnSODs are homologous and catalyze the disproportionation of superoxide through a cyclic (ping-pong) mechanism that involves O_2^- oxidation at M^{3+} followed by proton-induced O_2^- reduction at M^{2+}.[13,14,24] By poising the SOD redox potential half-way between the potentials at which superoxide is oxidized and reduced, the redox active metal center of SOD is able to both oxidize and reduce superoxide depending on the protonation states of the nearby residues and the oxidation state of the metal. In contrast to SOR, the SOD catalytic cycle does not re-

quire an external source of electrons. The redox potential of the SOD Fe^{2+}/Fe^{3+} couple is pH-dependent, and falls in the range from +0.03 to –0.31 V versus SCE.[14,30,31] The redox potential of the SOR Fe^{2+}/Fe^{3+} couple (reported range: 0.00 to –0.15 V versus SCE[29]) is similar to that of SOD, which indicates that the redox potential alone cannot be responsible for the two distinct reactions that are catalyzed. Differences in the protein structure might be responsible. Because the active site of SOR is close to the surface of the protein, a constant source of protons is available from the solvent.[17] In contrast, the active site of SOD is buried within the protein, which makes it easier to control proton delivery. The amount of protons available is perhaps limited when the metal ion is in its 3+ oxidation state so as to favor superoxide oxidation. The redox potential of superoxide (O_2^-) is highly dependent on the pH of the system and it is significantly easier to reduce under acidic conditions. At pH = 0, superoxide is reduced at a potential of +1.27 V versus SCE, whereas at pH = 7.5 and pH = 14, it is reduced at +0.83 and –0.041 V, respectively. Protons are probably used to raise the redox potential of superoxide and to drive its reduction by SOR. Given that superoxide reduction by SOR has been shown to occur via an inner sphere mechanism (vide infra), redox potentials are somewhat less important. However, they can influence the reaction pathway in a more indirect manner by determining the energy of the frontier (LUMO) orbitals.

Another barrier to SOD activity in SOR may involve the reorganizational energy that is required to convert from a six- to a five-coordinate structure.[10] In SOD, the ferric state is five-coordinate which would be amenable to re-reduction by superoxide via an inner sphere mechanism. In contrast, the resting state of SOR is a six-coordinate ferric site, and the low levels of superoxide present may not be able to effectively compete with the solvent (or the glutamate moiety) and bind to the metal ion.[10]

2.2 Enzymatic SOR Data

Superoxide has been shown to bind to the reduced Fe^{II} state of SOR at diffusion controlled rates ($> 10^9 \, \text{M}^{-1}\text{s}^{-1}$). The transfer of an electron from the metal ion to the bound substrate via an inner sphere pathway is then proposed to afford one or two Fe^{III}-peroxide intermediates, depending on the organism. These intermediates have been observed in pulse radiolysis experiments by electron absorption spectroscopy.[32,33] Consistent with an inner sphere pathway, exogenous ligands such as azide, nitric oxide, and cyanide have also been shown to bind to the iron site of SOR.[34–36] The putative peroxide intermediate displays a charge-transfer band at 600 ($\sim 3500 \, \text{M}^{-1}\text{cm}^{-1}$) nm and releases H_2O_2 at a rate of 40–50 s^{-1}.[32,33,37] The intense low-energy charge-transfer (CT) band was originally assigned as a combination peroxide/sulfur-to-metal charge-transfer transition,[32] but more recently it was suggested that this band is too low in energy for the peroxide to be involved.[38] This comes as somewhat of a surprise given that a number of

Fe^{III}–OOR (R = alkyl, H) model complexes have been synthesized which display a peroxide-to-metal CT band in the range 500–600 nm, at least when the iron is low-spin.[39] High-spin Fe^{III}–OOH species are extremely rare so there is less known about their spectroscopic properties. Upon the release of hydrogen peroxide from SOR, a nearby glutamate (Glu^{14} or Glu^{47}) coordinates to the iron center to afford the six-coordinate Fe^{III}-oxidized resting state.[17,23]

When the Glu^{47} residue is replaced with an alanine group (in an E47A SOR mutant of *D. baarsii*), a transient species is observed by resonance Raman spectroscopy upon the addition of hydrogen peroxide.[40] Stretches are observed for the O–O and Fe–O bonds at 850 and 438 cm^{-1}, respectively, which shift to 802 and 415 cm^{-1} in the ^{18}O-labeled spectrum.[40] Stretching frequencies in this range are consistent with a metal–peroxide species. Mössbauer parameters for this E47A intermediate enriched in ^{57}Fe include an isomeric shift of $\delta = 0.54(1)$ mm/s, with $\Delta E_Q = -0.80(5)$ mm/s, and an asymmetry parameter $\eta = 0.60(5)$ mm/s.[41] These data are consistent with the assignment of the H_2O_2-generated mutant species as a monomeric, high-spin ($S = 5/2$) ferric–peroxo. EPR, resonance Raman, and pulse radiolysis experiments have also been reported for the SOR isolated from *Treponema pallidum*.[42] Data consistent with the formation of an Fe^{III}–peroxo species was also observed upon treatment of the ferric or ferrous E48A mutant of *Treponema pallidum* SOR with H_2O_2. The same Fe^{III}–peroxo species could also be trapped in the corresponding wild-type, *D. baarsii* and *T. pallidum*, upon the addition of H_2O_2 but with much lower yields.[42] Mononuclear Fe^{III}–peroxide species have also been proposed, or identified, in the catalytic cycles of the antitumor drug bleomycin,[43] heme oxygenase,[44] cytochrome P450,[45–48] and Rieske dioxygenases.[49–51] DFT calculations comparing the stabilities of possible SOR intermediates suggest that a side-on peroxide would be much less stable than an end-on peroxide.[38]

Because two protons are needed to form H_2O_2, the active site's access to proton donors is a key consideration in the mechanism of SOR. In an attempt to identify potential proton donors, the pH-dependence of the spectroscopic and redox properties of WT and mutant (E47A and K48I) *D. baarsii* SOR has been recently examined.[52] With an increase in the pH, the $S{\rightarrow}Fe^{III}$ absorption band of center II exhibited an 84 nm shift from 644 to 560 nm in both the WT and the mutants. However, this shift occurred at a higher pH for the WT enzyme than for the mutants. This observation is consistent with the presence of an additional base other than Lys^{48} or Glu^{47} (Glu^{14} in *D. baarsii*), whose pK_a is influenced by the presence of these residues. The nearby Lys and Glu residues are highly conserved among SORs; however, only the Lys unit has been shown to noticeably influence the catalytic activity of the enzyme.[21,22] The Glu residue is proposed to play an important role in the structural reorganization that accompanies iron oxidation, whereas the positively charged Lys residue is believed to provide an electrostatic driving force that guides superoxide toward the reduced iron.[53] Resonance Raman spectroscopic data for K_2IrCl_6-oxidized WT and mutant *D. baarsii*

SOR, collected at various pHs, revealed a pH-dependent stretch that is consistent with the formation of a previously unidentified Fe^{III}–OH species.[54] Resonance Raman spectroscopy revealed that the stretches observed for these species (in the range v = 466–471 cm^{-1}) were sensitive to isotopic labeling with $H_2^{18}O$ or ^2H_2O buffer. This indicates that an oxygen atom that is derived from the solvent that contains an exchangeable proton is coordinated to the ferric site. This Fe^{III}–OH species (Figure 3) is proposed to be the previously observed base responsible for the pH-dependence of the SOR electronic absorption spectrum.[52] The protonated base (i.e. solvent = H_2O) is then presumed to be the second proton donor needed for H_2O_2 formation. This would allow the release of H_2O_2 with concomitant formation of the Fe^{III}–OH species (Figure 3).[54] Currently, the involvement of a solvent water molecule is proposed to only affect the second protonation step because Fe^{III}–OH formation cannot occur until H_2O_2 is released. The mechanism of H_2O_2 release, whether by an associative or dissociative process, however, is still unclear. The rate constant of H_2O_2 release by *D. baarsii* is estimated to be slow (< 5 s^{-1}) but has not been directly measured.[52] Furthermore, the dependence of this second protonation step on pH still requires further study.
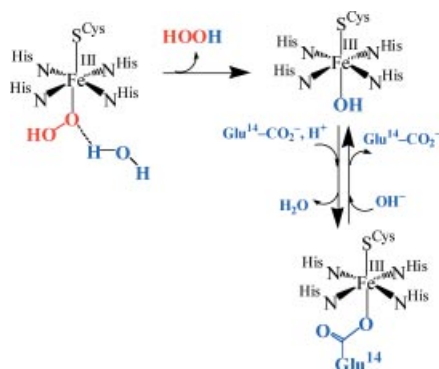

Figure 3. Proposed mechanism (see ref.[54]) for the solvent-induced H_2O_2 release from the putative Fe^{III}–OOH SOR intermediate, to initially afford a hydroxide-bound Fe^{III}–OH species, which converts to the glutamate-bound resting state Fe^{III}–OC(O)Glu under acidic conditions.

Nitric oxide (NO), a substrate analogue, has also been shown to bind to the active site of reduced *P. furiosus* SOR.[35] Reaction of ascorbate-reduced SOR with NO results in the reversible formation of a stable six-coordinate derivative with NO bound *trans* to the cysteinate ligand. EPR spectroscopy of the NO adduct shows a near-axial $S = 3/2$ ground state with $E/D = 0.06$ and $D = (12 \pm 2)$ cm^{-1}.[35] Resonance Raman studies indicate that the NO ligand is most likely in a bent conformation *trans* to the cysteinate ligand, with $v(N\equiv O)$ = 1721 cm^{-1}, $v(Fe–NO)$ = 475 cm^{-1}, and $v(Fe–S)$ = 291 cm^{-1}, confirmed by ^{15}NO and ^{34}S isotopic labeling.[35] The best electronic description of the $S = 3/2$ {FeNO}^{7} unit is that of a high-spin ($S = 5/2$) Fe^{III} center, antiferromagnetically coupled to an ($S = 1$) NO$^-$ anion, which indicates that NO oxidatively adds to the Fe^{II} center. These observations are consistent with the first step of the

SOR mechanism that involves oxidative addition of superoxide to form the proposed ferric peroxide intermediate.

To regenerate the Fe^{II}-active state, rubredoxin has been proposed to serve as an electron donor on the basis of genetic and biochemical evidence.[55] Rubredoxin is a small (ca. 6 kDa) iron-containing protein which contains a single [Fe(SCys)$_4$] site. These proteins are found in many anaerobic bacteria and archaea where they serve as one-electron carriers involved in numerous electron transfer chains. *D. vulgaris* rubredoxin has been found to efficiently catalyze the reduction of *D. vulgaris* 2Fe-SOD.[55] Rubredoxin has also been shown to act as an electron donor for neelaredoxin (a 1Fe-SOR) in vitro.[56] Additionally, rubredoxins have been shown to be reduced in vivo by NAD(P)H:rubredoxin oxidoreductase (NROR), and this reduction pathway was recently reconstituted in vitro with the use of recombinant proteins.[57]

2.3 Biomimetic Models of SOR

The spectroscopic characterization and isolation of Fe^{III}–peroxo complexes is extremely challenging because of their high reactivity, thermal instability, and photolability.[29,58] Que[39] (Figure 4) and Girerd[59] have reported the most extensively characterized set of synthetic nonheme iron peroxides. Both groups have shown that when ligated by nitrogen ligands, a side-on ferric peroxide [$Fe^{III}(\eta^2$-$O_2)$] will convert to an end-on ferric hydroperoxide species [$Fe^{III}(\eta^1$-OOH)] upon protonation.[60–63] In the published examples, the side-on peroxides are high-spin ($S = 5/2$), and the end-on hydroperoxides are low-spin ($S = 1/2$). The $v_{O–O}$ stretching frequencies of these side-on peroxides appear at higher energies than those of the corresponding end-on hydroperoxides. The $v_{Fe–O}$ stretch shifts to higher energies upon protonation, a spin-state change from $S = 5/2$ to $S = 1/2$ occurs, and, as predicted by Solomon,[64,65] the O–O bond weakens. Because protons are needed for SOR catalysis, any side-on peroxide that is possibly formed in wild-type SOR probably converts to an end-on hydroperoxide prior to the release of H_2O_2.
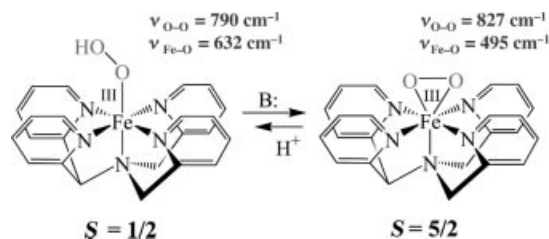

Figure 4. Que's synthetic end-on and side-on peroxide complexes, [(N$_4$Py)$Fe^{III}(\eta^2$-$O_2)$]$^+$ and [(N$_4$Py)$Fe^{III}(\eta^1$-OOH)]$^{2+}$, and their respective vibrational data and spin-states.

None of the synthetic complexes described above contain thiolate ligands. An obvious question related to SOR concerns how a thiolate sulfur would affect H_2O_2 formation and release. The *trans* positioning of the thiolate moiety in SOR has been suggested to provide a pathway for electron delivery to the iron site. Additionally, the *trans*-effect of the

thiolate ligand would cause the Fe–O bond to become labile, which favors peroxide release.[34] As established for porphyrin-containing systems,[66–68] a thiolate would be expected to perturb the spectroscopic and magnetic properties of Fe^{III}-peroxide species and their preferred reaction pathways relative to those not containing a thiolate ligand. The correlation between the peroxide binding mode, spin-state, and vibrational parameters, established for nitrogen-ligated nonheme iron systems,[39] would not necessarily hold true for thiolate ligated systems. For example, the π-donor sulfur ligand may favor a high-spin Fe^{III}–OOH species with a weaker Fe–O bond, which would then favor peroxide release (vide infra). In order to confirm these hypotheses, thiolate-ligated Fe^{III}–OOH complexes are needed. Thiolate-ligated Fe^{III}–OOH species are, however, difficult synthetic targets because thiolates tend to reduce Fe^{III}, are easily oxidized by peroxides, and form μ-SR bridged dimers.[29]

Halfen and coworkers have successfully modeled the square pyramidal structure of reduced SOR with a pyridyl appended diazacyclooctane ligand (Figure 5).[69] Aromatic thiolate groups coordinate to the apical position of the reduced, high-spin ($S = 2$) complex *trans* to an open coordination site, which affords a fairly accurate structural model of the reduced form of SOR (SOR$_{red}$), $[L_8py_2Fe(SC_6H_4$-m-$CH_3)]^+$ (**1**). Although **1** is stereochemically very similar to SOR$_{red}$, its electronic structure is notably different.[70] Electronic absorption, magnetic circular dichroism (MCD), and variable-temperature variable-field MCD (VTVH-MCD) spectroscopy, in conjunction with density functional theory (DFT) and semiemperical INDO/S-CI calculations, showed that the π-acceptor pyridine ligands stabilize the reduced state of **1** relative to that of SOR. This, coupled with the poor sigma-donor properties of the aromatic thiolate compared with those of alkyl thiolate cysteinates, causes a blue-shift in the S→Fe^{II} CT manifold of **1** by 9,000 cm^{-1} relative to that of the enzyme. Initially, the oxidation of **1** was found to be irreversible, which resulted in the formation of disulfides.[69] No reaction was reported with superoxide. More recently, tBuOOH was shown to react with **1** to afford a high-spin ($S = 5/2$) ferric alkylperoxide complex, $[L_8py_2$-$Fe(SC_6H_4$-m-$CH_3)(OOR)]^+$ (**2**).[71] The resonance Raman spectrum of **2** shows vibrations that are consistent with an end-on Fe^{III}–OOR species.[71]
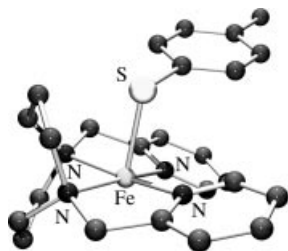

Figure 5. Halfen's thiolate-ligated, pyridyl-appended diazacyclooctane iron complex $[L_8py_2Fe(SC_6H_4$-m-$CH_3)]^+$ (**1**, see ref.[69]).

In 2001, Shearer and Kovacs showed that when the thiolate sulfur is incorporated into a multidentate ligand, biomimetic SOR reactivity is observed.[72,73] This occurs even though the thiolate moiety is coordinated *cis* to the open site and not *trans* to the open site as in the enzyme. In the model, five-coordinate thiolate-ligated $[Fe^{II}\{S^{Me2}N_4$-$(tren)\}]^+$ (**3**, Figure 6) reacts with superoxide (solubilized as an 18-crown-6-K$^+$ salt in THF) to afford H_2O_2 and solvent-ligated $[Fe^{III}\{S^{Me2}N_4(tren)\}(solv)]^{2+}$ (solv = MeO$^-$ or MeCN). The reaction requires a proton source (such as MeOH or a trace amount of water from MeCN) and does not occur in rigorously dried THF. At low temperatures ($\leq$ –78 °C), a transient hydroperoxide intermediate, $[Fe^{III}\{S^{Me2}N_4(tren)(OOH)\}]^+$ (**4**, Figure 7), is observed that has been characterized by electronic absorption, EPR, IR, and XAS spectroscopies.[73] The orange peroxide intermediate displays a charge-transfer band at 452 (2780 M^{-1}cm^{-1}) nm and is low-spin ($S = 1/2$; $g_\parallel = 2.14$, $g_\perp = 1.97$). Peroxide bound **4** displays a Fermi doublet in the IR spectrum at 788 and 781 cm^{-1} which collapses to a singlet at 784 cm^{-1} upon deuteration with D_2O.[73] A new $\nu_{O–O}$ stretch is observed at 752 cm^{-1} when ^{18}O-labeled superoxide is used, which confirms the $\nu_{O–O}$ assignment. This 31 cm^{-1} shift is close to that predicted (44 cm^{-1}) for a diatomic oxygen species. Fits to the EXAFS data of **4** required the addition of a new short Fe–O bond at 1.86(3) Å that is not present in either the Fe^{II} precursor (**3**) or the MeO$^-$-bound product.[73] The XANES spectrum is consistent with a six-coordinate oxidized Fe^{III} intermediate. Addition of an outer sphere oxygen at 2.79(6) Å improved the EXAFS fits slightly. The small Debye-Waller factor that is associated with this outer sphere oxygen suggests that it is highly ordered, possibly due to H-bonding between the hydroperoxide and the *cis* thiolate sulfur. This hydrogen bonding may also help explain the shift in the S→Fe^{III} charge-transfer band to higher energies in the absorption spectrum relative to that of the enzyme (452 nm versus 600 nm). More likely, notable differences that distinguish **4** from the enzyme intermediate are responsible. These differences include the low-spin state and the *cis* positioning of the thiolate group relative to the peroxide of **4** compared with the high-spin state and the *trans* positioning of the thiolate group in the enzyme intermediate. Hydrogen peroxide is released from **4** at a rate of 65(1) s^{-1} (at 298 K), which is comparable to the rate of H_2O_2 release in the SOR enzyme, and a stable solvent-bound species $[Fe^{III}\{S^{Me2}N_4(tren)(solv)\}]^{2+}$ is afforded. Together, these data are consistent with a mechanism that involves the inner sphere oxidative addition of superoxide to $[Fe^{II}\{S^{Me2}N_4(tren)\}]^+$ to form an end-on $Fe^{III}(\eta^1$-OOH) intermediate, $[Fe^{III}\{S^{Me2}N_4(tren)(OOH)\}]^+$. This represents the first example of a thiolate-ligated peroxide species.

The role of protons in the formation of Fe^{III}–peroxide model complex **4** has been examined in more detail in order to help identify viable proton donors in the SOR mechanism.[74] The source of the first proton in SOR is unclear and is dependent on the local pH. Under acidic conditions, ^{14}Glu-CO_2H has been proposed to serve as the proton donor. The solvent was shown to be capable of providing protons in *D. baarsii* SOR.[52] A highly conserved Lys-NH_3^+ residue (^{15}Lys or ^{48}Lys), essential for the catalytic activity of the enzyme, has been shown to affect rates

Figure 6. Kovacs' reactive *cis*-thiolate-ligated iron complex [Fe^{II}{S^{Me2}N$_4$(tren)}]$^+$ (**3**), which has been shown to convert superoxide to H$_2$O$_2$ via a Fe^{III}–OOH intermediate in a proton-dependent mechanism (see refs.[73,74]).

Figure 7. The hydroperoxide-bound intermediate [Fe^{III}{S^{Me2}N$_4$-(tren)(OOH)}]$^+$ (**4**) shown to be involved in superoxide reduction by reduced **3** (see ref.[73]).

of H$_2$O$_2$ formation, which implies its involvement in the mechanism.[12,23] In order to explore this, the rate of formation of the synthetic peroxide intermediate [Fe^{III}{S^{Me2}N$_4$(tren)(OOH)}]$^+$ (**4**) was examined in dry THF with a variety of proton donors including HOAc and NH$_4^+$ as analogs for glutamic acid and lysine.[74] No reaction occurs between pre-purified **3** and superoxide in rigorously dried solvents, which rules out a mechanism that involves H$^+$ or H-atom abstraction from the ligand. The rates of formation of **4** are also dependent on the pK_a of the proton donor: for the reaction to occur at comparable rates, the concentration of EtOH must be ca. 500 times higher than that of NH$_4^+$.[74] Although the pK_a's (both relative and absolute) of these proton donors are likely to differ dramatically in THF (versus H$_2$O), and at low temperatures, the observation that EtOH will serve as a proton source to afford **4** suggests that the initial protonation site is rather basic. Additionally, superoxide is quite basic in aprotic solvents [pK_a(HO$_2$) = 25.3 in DMF],[75] which indicates that these observations do not rule out a mechanism that involves the initial protonation of the superoxide anion prior to its oxidative addition to the metal ion. Protonated superoxide, HO$_2$, is a more potent oxidant than O$_2^-$, and the kinetic experiments needed to distinguish between these mechanisms are ongoing.

Subsequent addition of a second proton to **4** results in the release of hydrogen peroxide to afford the solvent-bound complex [Fe^{III}{S^{Me2}N$_4$(tren)(solv)}]$^{2+}$.[74] The second protonation step requires strong acids such as HOAc, HBF$_4$, or HClO$_4$ (Figure 8). Weaker acids (e.g. NH$_4^+$, a

lysine analogue, and MeOH) do not release H$_2$O$_2$ from **4** in MeOH at reasonable rates at –78 °C. Noncoordinating acids (HBF$_4$, HClO$_4$) cleanly afford a common purple intermediate, [Fe^{III}{S^{Me2}N$_4$(tren)(MeOH)}]$^{2+}$ (**5**). Acetic acid also reacts with **4** to form **5** (Figure 8), which then converts to acetate-bound [Fe^{III}{S^{Me2}N$_4$(tren)(OAc)}]$^+$ at ambient temperature. Reaction rates are dependent on the pK_a of the proton donor and are complete in seconds with strong acids (HBF$_4$, HClO$_4$) versus hours with HOAc. Glutamic acid-promoted H$_2$O$_2$ release by SOR could occur via a similar mechanism involving a solvent-bound intermediate. The common MeOH-bound intermediate **5** observed in all three reactions suggests that H$_2$O$_2$ release occurs via a proton-induced dissociative mechanism. An associative mechanism that involves nucleophilic displacement is ruled out because NH$_4^+$OAc$^-$ does not release H$_2$O$_2$ from **4**.
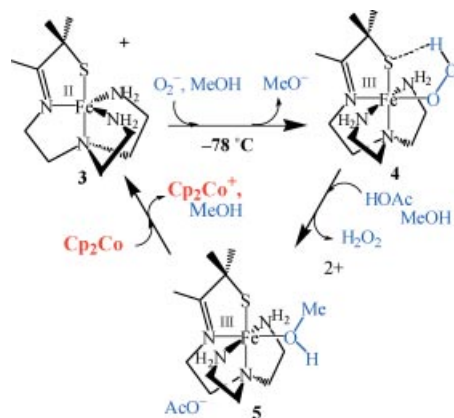

Figure 8. The catalytic cycle involving [Fe^{II}{S^{Me2}N$_4$(tren)}]$^+$ (**3**) promoted reduction of superoxide, which involves sequential protonation and Cp$_2$Co promoted reduction to afford H$_2$O$_2$.

To mimic the reduction of the oxidized Fe^{III} state of SOR, and to complete the catalytic cycle, cobaltacene was added as a source of electrons to oxidized solvent-bound **5**. This resulted in the regeneration of reduced [Fe^{II}{S^{Me2}N$_4$(tren)}]$^+$ (**3**), which subsequently reacts with additional superoxide to regenerate the peroxide intermediate (Figure 8). Eight turnovers have been achieved in this stepwise manner.[74] The catalytic activity is believed to be limited because of the decomposition of the catalyst by H$_2$O$_2$. Conditions are currently being optimized to remove the H$_2$O$_2$ that is formed in situ, in hopes of increasing the lifetime of the catalyst.

Cyanide, azide, and acetate all bind to oxidized solvent-bound [Fe^{III}{S^{Me2}N$_4$(tren)(MeCN)}]$^{2+}$ to afford models for the CN$^-$-inhibited, N$_3^-$-bound, and Glu-bound resting state of SOR.[76] Cyanide and azide do not bind to reduced **3**, and do not prevent **3** from stoichiometrically reducing superoxide. Azide- and acetate-coordinated [Fe^{III}{S^{Me2}N$_4$-(tren)(N$_3$)}]$^+$ (**6**) and [Fe^{III}{S^{Me2}N$_4$(tren)(OAc)}]$^+$ (**7**) each have an $S = 1/2$ ground state with a thermally accessible higher spin state. Cyanide-bound [Fe^{III}{S^{Me2}N$_4$(tren)-(CN)}]$^+$ (**8**), on the other hand, is $S = 1/2$ over a wide temperature range (2–300 K). Cyanide also dramatically alters the magnetic properties of SOR: CN-SOR is low-spin (S =

1/2), whereas N_3-SOR and Glu-SOR are high-spin ($S = 5/2$). These differences in spin-state do not come as a surprise given the differences in ligand field strengths of N_3^- versus RCO_2^- versus CN^-. The redox properties of these model complexes show a similar trend. Azide- and OAc-ligated **6** and **7** are reduced at comparable potentials of –410 and –335 mV (versus. SCE), respectively, whereas CN-ligated **8** is reduced at a much more anodic potential of –805 mV versus SCE.[76] If cyanide were to cause an anodic shift in the redox potential of SOR by approximately the same amount ($|\Delta E| \geq 470$ mV), then the reduction potential of the catalytic iron center would fall well-below those of its biological reductants (center I, –236 mV versus SCE; rubredoxin, reported range –191 to –291 versus SCE). Thus, cyanide by preventing the enzyme from turning over because it prevents the regeneration of the reduced, catalytically active Fe^{2+} state of SOR. There is no data to support such a mechanism with the SOR enzyme; however, cyanide has been shown to inhibit superoxide dismutase in this manner.[77] Given that electron transfer plays a prominent role in SOR chemistry, inhibition may occur if these redox processes are interfered with.

With the use of a rigid macrocyclic ligand with tertiary amines and an appended alkyl thiolate, Halfen was more recently able to synthesize a high-spin ($S = 2$) SOR$_{red}$ model, [Fe^{II}(Me$_3$-cyclam-EtS)]$^+$ (**9**, Figure 9), which displays an absorption spectrum similar to that reported for the reduced SOR enzyme (SOR$_{red}$). This suggests that this model accurately mimics key elements of the electronic structure of the enzyme's active site, specifically its highly covalent Fe–S π- and σ-bonding interactions.[70] The geometry of **9** is distorted from the square pyramidal architecture, which results in a shift of the redox active orbital from the equatorial N_4 plane, as it occurs in SOR, to an axial (d_{yz}) position. Although **9** does not appear to react with superoxide, it reacts with either H_2O_2 in MeOH or *m*-chloroperbenzoic acid (*m*CPBA) in the presence of a base at –60 °C to afford a high-valent Fe^{IV}=O species, [(Me$_3$-cyclam-EtS)Fe^{IV}(O)]$^+$ (**10**).[78] The Mössbauer parameters associated with ^{57}Fe-enriched **10** ($\delta = 0.19$ mm/s; $\Delta E_Q = 0.22$ mm/s) are consistent with related Fe^{IV}=O cyclam-ligated complexes {i.e. [(Me$_4$-cyclam)Fe^{IV}(O)(MeCN)]$^{2+}$} that have been crystallographically characterized,[79] but which do not contain a thiolate sulfur in the coordination sphere. Bond lengths of **10**, as determined by EXAFS and DFT methods, include a short Fe–O bond of 1.70(2) Å, 3 Fe–N/O bonds of 2.09(2) Å, and one Fe–S bond of 2.33(2) Å. The formation of **10** presumably occurs via the cleavage of the O–O bond of a transient peroxide species. Thus, the reactivity of **9** appears to better mimic that of the heme enzyme cytochrome P450[45] rather than SOR. The tertiary amines possibly contribute to this (vide infra).

If secondary amines are incorporated into **9** in place of the tertiary amines and an extra methylene is inserted into the apical arm, the resulting thiolate-ligated complex [Fe^{II}(cyclam)-PrS]$^+$ (**11**, Figure 10) reacts with superoxide (solubilized as an 18-crown-6 salt in THF) in CH_2Cl_2 to form a metastable burgundy-colored peroxide species
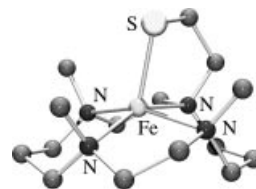

Figure 9. Halfen's SOR$_{red}$ model, [Fe^{II}(Me$_3$-cyclam-EtS)]$^+$ (**9**), which has been shown[70,78] to react with *m*CPBA to afford a high-valent Fe^{IV}=O species, [(Me$_3$-cyclam-EtS)Fe^{IV}(O)]$^+$ (**10**).

[$\lambda_{max} = 530(1350)$ nm], [Fe^{III}(cyclam-PrS)(OO(H))]$^+$ (**12**), upon the addition of a proton donor (e.g. MeOH).[80] This intermediate is high-spin ($g = 7.72, 5.40, 4.15$), and displays ν_{O-O}, ν_{Fe-O}, and ν_{Fe-S} stretches in the resonance Raman spectrum at 891 cm^{-1} (a Fermi doublet), 419 cm^{-1}, and 352 cm^{-1}, respectively.[80] The ν_{O-O} and ν_{Fe-O} peaks shift to 856 cm^{-1} and 400 cm^{-1}, respectively, upon the introduction of an isotopic label derived from $K^{18}O_2$ (50% enriched). The ν_{Fe-O} stretch of **12** (419 cm^{-1}) is unusually low, and the ν_{O-O} stretch (891 cm^{-1}) is unusually high, compared with other reported synthetic nonheme iron peroxo species (reported range: 450–639 cm^{-1} for ν_{Fe-O} and 820–860 cm^{-1} for ν_{O-O}),[39] but compares well with that of the only reported SOR peroxide species ($\nu_{Fe-O} = 438$ cm^{-1} and $\nu_{O-O} = 850$ cm^{-1}).[40] These vibrational data, along with the calculated force constant ($k_{Fe-O} = 1.20$ mdynes cm^{-2}), indicate that *the Fe–O(peroxide) bond is significantly weakened upon the introduction of a trans thiolate into the coordination sphere*. An increased lability of the Fe–O bond supports this conclusion. Peroxide-ligated **12** releases H_2O_2 much more rapidly (on the order of minutes) than does *cis* thiolate ligated [Fe^{III}{$S^{Me2}N_4$(tren)(OOH)}]$^+$ (**4**, $t_{1/2} = 69$ h), and represents the first example of a *trans* thiolate-ligated Fe^{III}-peroxo.[80] The more rapid rate of H_2O_2 release from **12** versus that of **4** suggests that the *trans* positioning of the thiolate in **12** (as well as in the SOR enzyme) plays an important functional role in the promotion of the rapid release of H_2O_2 and perhaps explains why this stereochemical arrangement is utilized by the enzyme.
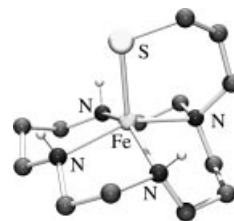

Figure 10. Kovacs' secondary amine-ligated SOR$_{red}$ model, [Fe^{II}(cyclam)-PrS]$^+$ (**11**), which was recently shown[80] to react with superoxide to afford H_2O_2 via the peroxo intermediate [Fe^{III}(cyclam-PrS)(OO(H))]$^+$ (**12**).

2.4 SOR versus Cytochrome P450

Cytochrome P450 is a heme (i.e. porphyrin-containing) iron enzyme involved in the metabolism of drugs and xenobiotics, the biosynthesis of key steroid hormones, and the

conversion of polyunsaturated fatty acids to biologically active molecules.[45] Like SOR, the P450 catalytic cycle proceeds via an end-on hydroperoxide intermediate (Figure 11).[45] However, the subsequent reactivity of the hydroperoxide is different in each case and has been shown to be dependent on the site of protonation as well as the spin-state of the molecule.[64,81–83] In SOR, Fe^{III}–OOH is presumably protonated at the proximal oxygen (the oxygen bound to the metal ion) to weaken the Fe–O bond, release hydrogen peroxide, and generate the oxidized Fe^{III} state. In P450, protonation occurs at the distal oxygen, which polarizes the O–O bond, liberates H_2O, and affords a high-valent $Fe^{IV}=O$ π cation radical.[45] Initially, this difference in reactivity was ascribed to the presence of a porphyrin ring in cytochrome P450.[48,84] The highly conjugated, negatively charged porphyrin is able to delocalize excess positive charge, which allows for the formation of high-valent "$Fe^V=O$" in this environment. However, Que et al. have observed $Fe^{IV}=O$ outside of a porphyrin environment and have definitive X-ray crystallographic evidence for examples of these species.[79] Another explanation for the differences in reactivity of SOR versus P450 may involve differences in the spin-state of the hydroperoxide intermediate.[29] The low-spin Fe–OOH of P450 and synthetic analogues have been shown to favor a reaction pathway that involves cleavage of the O–O bond.[64,82,85] In contrast, a high-spin Fe-peroxide ($S = 5/2$) would favor a reaction pathway that involves cleavage of the Fe–O bond because it would possess populated antibonding σ*(Fe–O) orbitals. The peroxide species formed upon the reaction of the E47A SOR mutant with H_2O_2 is high-spin ($S = 5/2$); however, this may not be true for the native enzyme intermediate. Recent calculations suggest that the peroxide-bound SOR intermediate is low-spin ($S = 1/2$);[38] however, there is no experimental evidence to confirm this. There is no evidence for oxygenase activity with SOR, which suggests that O–O bond cleavage does not occur, and reduced Fe^{II}-SOR is believed to be unreactive towards O_2.
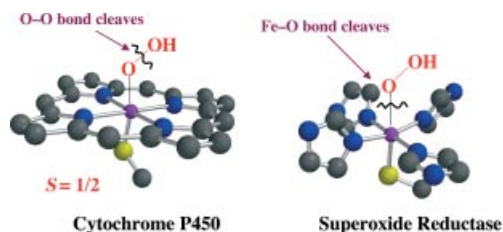

Figure 11. The hydroperoxide intermediates formed during catalysis by the heme iron oxygenase enzyme cytochrome P450 and non-heme iron enzyme SOR, which shows how their reaction pathways (i.e. O–O versus Fe–O bond cleavage) differ.

3. Perspective

The accumulation of biochemical and modeling data has begun to generate a clearer picture of the mechanism of superoxide reduction by SOR, but some questions still remain. How SOR is able to selectively reduce superoxide

rather than disproportionate O_2^- to O_2 and H_2O_2 (i.e. SOD activity) is not completely understood. Furthermore, how O–O bond cleavage is avoided in SOR remains unclear. The spin-state of the intermediate peroxide seems to play an important role in determining whether the Fe–O or O–O bond cleaves. It is still unknown whether the peroxide intermediate that is observed during catalysis of wild-type SOR is high- or low-spin. If such an intermediate can be detected in wild-type SOR, then resonance Raman experiments of the peroxide should be carried out with doubly-labeled superoxide, $^{16}O^{18}O^-$, in order to conclusively determine whether this intermediate contains an end-on or a side-on peroxide.

The position of the thiolate (trans versus cis to the peroxide) does not appear to be critical for the reduction of superoxide given that a five-coordinate $Fe^{II}N_4S$ SOR model complex with the thiolate positioned cis to the open site has been shown to reduce superoxide. However, the mechanism of superoxide reduction, and the rate of superoxide binding and hydrogen peroxide release, is likely to be affected by the position of the sulfur moiety. When a trans thiolate sulfur is incorporated into a macrocyclic five-coordinate $Fe^{II}N_4S$ SOR model complex, the Fe^{III}–OOH intermediate is high-spin and hydrogen peroxide is released more rapidly. The ν_{Fe-O} is also lower than any iron peroxide, with the exception of the SOR-peroxide. This suggests that the trans thiolate weakens the Fe–O bond and favors H_2O_2 release. However, one other trans thiolate-ligated five-coordinate non-heme $Fe^{II}N_4S$ model complex has been reported that does not reduce superoxide, yet reacts with H_2O_2 to afford a high-valent $Fe^{IV}=O$ species via cleavage of the O–O bond analogous to that observed in P450. Clearly, more than just the stereochemical relationship between the thiolate and the peroxide is important in the determination of the favored reaction pathway. A more thorough investigation that involves a series of structurally-related compounds is needed to correlate Fe–O (versus O–O) bond-cleaving properties with the spin-state of the molecule, the positioning of the thiolate sulfur (cis versus trans to the peroxide), redox properties, as well as proximal peroxide oxygen basicity.

Acknowledgments

[1] J. A. Imlay, *J. Biol. Inorg. Chem.* **2002**, *7*, 659–663.

[2] A. C. Maritim, R. A. Sanders, J. B. Watkins III, *J. Biochem. Mol. Toxicol.* **2003**, *17*, 24–38.

[3] G. Fortunato, A. Pastinese, M. Intrieri, M. M. Lofrano, G. Gaeta, M. B. Censi, A. Boccalatte, F. Salvatore, L. Sacchetti, *Clin. Biochem.* **1997**, *30*, 569–571.

[4] P. A. Kocaturk, M. C. Akbostanci, F. Tan, G. O. Kavas, *Pathophysiology* **2000**, *7*, 63–67.

[5] Y. Ihara, M. Chuda, S. Kuroda, T. Hayabara, *J. Neurol. Sci.* **1999**, *170*, 90–95.

[6] M. E. De Leo, S. Borrello, M. Passantino, B. Palazzotti, A. Mordente, A. Daniele, V. Filippini, T. Galeotti, C. Masullo, *Neurosci. Lett.* **1998**, *250*, 173–176.

[7] S. L. Marklund, R. Adolfsson, C. G. Gottfries, B. Winblad, *J. Neurol. Sci.* **1985**, *67*, 319–325.

[8] Y. Toh, S. Kuninaka, M. Mori, T. Oshiro, Y. Ikeda, H. Nakashima, H. Baba, S. Kohnoe, T. Okamura, K. Sugimachi, *Oncology* **2000**, *59*, 223–228.

[9] R. H. Burdon, *Free Rad. Biol. Med.* **1995**, *18*, 775–794.

[10] D. M. Kurtz Jr, *Acc. Chem. Res.* **2004**, *37*, 902–908.

[11] V. Nivière, M. Fontecave, *J. Biol. Inorg. Chem.* **2004**, *9*, 119–123.

[12] D. M. Kurtz Jr, *J. Inorg. Biochem.* **2006**, *100*, 679–693.

[13] A.-F. Miller, *Curr. Op. Chem. Biol.* **2004**, *8*, 162–168.

[14] T. A. Jackson, T. C. Brunold, *Acc. Chem. Res.* **2004**, *37*, 461–470.

[15] F. Auchere, F. Rusnak, *J. Biol. Inorg. Chem.* **2002**, *7*, 664–667.

[16] M. W. W. Adams, F. E. Jenney Jr, M. D. Clay, M. K. Johnson, *J. Biol. Inorg. Chem.* **2002**, *7*, 647–652.

[17] A. P. Yeh, Y. Hu, F. E. Jenney Jr, M. W. W. Adams, D. C. Rees, *Biochemistry* **2000**, *39*, 2499–2508.

[18] A. V. Coelho, P. Matias, V. Fulop, A. Thompson, A. Gonzalez, M. A. Carrondo, *J. Biol. Inorg. Chem.* **1997**, *2*, 680–689.

[19] T. Santos-Silva, J. Trincao, A. L. Carvalho, C. Bonifacio, F. Auchere, P. Raleiras, I. Moura, J. J. G. Moura, M. J. Romao, *J. Biol. Inorg. Chem.* **2006**, *11*, 548–558.

[20] V. Adam, A. Royant, V. Niviere, F. P. Molina-Heredia, D. Bourgeois, *Structure* **2004**, *12*, 1729–1740.

[21] J. P. Emerson, D. E. Cabelli, D. M. Kurtz Jr, *Proc. Natl. Acad. Sci. USA* **2003**, *100*, 3802–3807.

[22] J. P. Emerson, E. D. Coulter, D. E. Cabelli, R. S. Phillips, D. M. Kurtz Jr, *Biochemistry* **2002**, *41*, 4348–4357.

[23] M. Lombard, C. Houee-Levin, D. Touati, M. Fontecave, V. Niviere, *Biochemistry* **2001**, *40*, 5032–5040.

[24] Fridovich, *Acc. Chem. Res.* **1972**, *5*, 321–326.

[25] F. E. Jenney Jr, M. F. J. M. Verhagen, X. Cui, M. W. W. Adams, *Science* **1999**, *286*, 306–309.

[26] A.-F. Miller in *Handbook of Metalloproteins* (Eds.: A. Messerschmidt, R. M. T. Poulos, K. Wieghardt), Wiley, New York, **2001**, vol. 1, pp. 668–682.

[27] J. Wuerges, J.-W. Lee, Y.-I. Yim, H.-S. Yim, S.-O. Kang, K. D. Carugo, *Proc. Natl. Acad. Sci. USA* **2004**, *101*, 8569–8574.

[28] E. L. Hegg, L. Que Jr, *Eur. J. Biochem.* **1997**, *250*, 625–629.

[29] J. A. Kovacs, *Chem. Rev.* **2004**, *104*, 825–848.

[30] C. K. Vance, A.-F. Miller, *Biochemistry* **2001**, *40*, 13079–13087.

[31] C. K. Vance, A.-F. Miller, *J. Am. Chem. Soc.* **1998**, *120*, 461–467.

[32] E. D. Coulter, J. P. Emerson, D. M. Kurtz Jr, D. E. Cabelli, *J. Am. Chem. Soc.* **2000**, *122*, 11555–11556.

[33] V. Nivière, M. Lombard, M. Fontecave, C. Houee-Levin, *FEBS Lett.* **2001**, *497*, 171–173.

[34] M. D. Clay, F. E. Jenney Jr, P. L. Hagedoorn, G. N. George, M. W. W. Adams, M. K. Johnson, *J. Am. Chem. Soc.* **2002**, *124*, 788–805.

[35] M. Clay, C. A. Cosper, F. E. Jenney Jr, M. W. W. Adams, M. K. Johnson, *Proc. Natl. Acad. Sci. USA* **2003**, *100*, 3796–3801.

[36] M. D. Clay, T.-C. Yang, F. E. Jenney Jr, I. Y. Kung, C. A. Cosper, R. Krishnan, D. M. Kurtz Jr, M. W. W. Adams, B. M. Hoffman, M. K. Johnson, *Biochemistry* **2006**, *45*, 427–438.

[37] D. M. Kurtz, E. D. Coulter, *J. Biol. Inorg. Chem.* **2002**, *7*, 653–658.

[38] R. Silaghi-Dumitrescu, I. Silaghi-Dumitrescu, E. D. Coulter, D. M. Kurtz Jr, *Inorg. Chem.* **2003**, *42*, 446–456.

[39] G. Roelfes, V. Vrajmasu, K. Chen, R. Y. N. Ho, J.-U. Rohde, C. Zondervan, R. M. Crois, E. P. Schudde, M. Lutz, A. L. Spek, R. Hage, B. L. Feringa, E. Munck, L. Que Jr, *Inorg. Chem.* **2003**, *42*, 2639–2653.

[40] C. Mathe, T. A. Mattioli, O. Horner, M. Lombard, M. J. Latour, M. Fontecave, V. Niviere, *J. Am. Chem. Soc.* **2002**, *124*, 4966–4967.

[41] O. Horner, J.-M. Mouesca, J.-L. Oddou, C. Jeandy, V. Niviere, T. A. Mattioli, C. Mathe, M. Fontecave, P. Maldivi, P. Bonville, J. A. Halfen, J.-M. Latour, *Biochemistry* **2004**, *43*, 8815–8825.

[42] C. Mathé, V. Nivière, C. Houée-Levin, T. A. Mattioli, *Biophys. Chem.* **2006**, *119*, 38–48.

[43] R. M. Burger, *Struct. Bonding* **2000**, *97*, 287–303.

[44] P. R. Ortiz de Montellano, *Acc. Chem. Res.* **1998**, *31*, 543–549.

[45] I. G. Denisov, T. M. Makris, S. G. Sligar, I. Schlichting, *Chem. Rev.* **2005**, *105*, 2253–2277.

[46] I. Schlichting, J. Berendzen, K. Chu, A. M. Stock, S. A. Maves, D. E. Benson, R. M. Sweet, D. Ringe, G. A. Petsko, S. G. Sligar, *Science* **2000**, *287*, 1615–1622.

[47] G. H. Loew, D. L. Harris, *Chem. Rev.* **2000**, *100*, 407–419.

[48] M. Sono, M. P. Roach, E. D. Coulter, J. H. Dawson, *Chem. Rev.* **1996**, *96*, 2841–2887.

[49] M. D. Wolfe, J. V. Parales, D. T. Gibson, J. D. Lipscomb, *J. Biol. Chem.* **2001**, *276*, 1945–1953.

[50] A. Karlsson, J. V. Parales, R. E. Parales, D. T. Gibson, H. Eklund, S. Ramaswamy, *Science* **2003**, *299*, 1039–1042.

[51] L. Que Jr, R. Y. N. Ho, *Chem. Rev.* **1996**, *96*, 2607–2624.

[52] V. Nivière, M. Asso, C. O. Weill, M. Lombard, B. Guigliarelli, V. Favaudon, C. Houée-Levin, *Biochemistry* **2004**, *43*, 808–818.

[53] C. Berthomieu, F. Dupeyrat, M. Fontecave, A. Verméglio, V. Nivière, *Biochemistry* **2002**, *41*, 10360–10368.

[54] C. Mathé, V. Nivière, T. A. Mattioli, *J. Am. Chem. Soc.* **2005**, *127*, 16436–16441.

[55] E. D. Coulter, D. M. Kurtz, *Arch. Biochem. Biophys.* **2001**, *394*, 76–86.

[56] J. V. Rodrigues, I. A. Abreu, L. M. Saraiva, M. Teixeira, *Biochem. Biophys. Res. Commun.* **2005**, *329*, 1300–1305.

[57] A. M. Grunden, F. E. Jenney Jr, K. Ma, M. Ji, M. V. Weinberg, M. W. W. Adams, *Appl. Environ. Microbiol.* **2005**, *71*, 1522–1530.

[58] M. Costas, M. P. Mehn, M. P. Jensen, L. Que Jr, *Chem. Rev.* **2004**, *104*, 939–986.

[59] J.-J. Girerd, F. Banse, A. J. Simaan, *Struct. Bonding* **2000**, *97*, 145–177.

[60] G. Roelfes, M. Lubben, K. Chen, R. Y. N. Ho, A. Mettsma, S. Genseberger, R. M. Hermant, R. Hage, S. K. Mandal, V. G. Young Jr, Y. Zang, H. Kooijman, A. L. Spek, L. Que Jr, B. L. Feringa, *Inorg. Chem.* **1999**, *38*, 1929–1936.

[61] A. J. Simaan, F. Banse, P. Mialane, A. Boussac, S. Un, T. Karger-Grisel, G. Bouchoux, J.-J. Girerd, *Eur. J. Inorg. Chem.* **1999**, 993–996.

[62] R. Y. N. Ho, G. Roelfes, B. L. Feringa, L. Que Jr, *J. Am. Chem. Soc.* **1999**, *121*, 264–265.

[63] A. J. Simaan, F. Banse, J.-J. Girerd, K. Wieghardt, E. Bill, *Inorg. Chem.* **2001**, *40*, 6538–6540.

[64] N. Lehnert, R. Y. N. Ho, L. Que Jr, E. I. Solomon, *J. Am. Chem. Soc.* **2001**, *123*, 12802–12816.

[65] N. Lehnert, R. Y. N. Ho, L. Que Jr, E. I. Solomon, *J. Am. Chem. Soc.* **2001**, *123*, 8271–8290.

[66] S.-I. Adachi, S. Nagano, K. Ishimori, Y. Watanabe, I. Morishima, T. Egawa, T. Kitagawa, R. Makino, *Biochemistry* **1993**, *32*, 241–252.

[67] J. T. Groves, Y. Watanabe, *J. Am. Chem. Soc.* **1988**, *110*, 8443–8452.

[68] K. Yamaguchi, Y. Watanabe, I. Morishima, *J. Am. Chem. Soc.* **1993**, *115*, 4058–4065.

[69] J. A. Halfen, H. L. Moore, D. C. Fox, *Inorg. Chem.* **2002**, *41*, 3935–3943.

[70] A. T. Fiedler, H. L. Halfen, J. A. Halfen, T. C. Brunold, *J. Am. Chem. Soc.* **2005**, *127*, 1675–1689.

[71] M. R. Bukowski, H. L. Halfen, T. A. van der Berg, J. A. Halfen, L. Que Jr, *Angew. Chem. Int. Ed.* **2005**, *44*, 584–587.

[72] J. Shearer, J. Nehring, W. Kaminsky, J. A. Kovacs, *Inorg. Chem.* **2001**, *40*, 5483–5484.

[73] J. Shearer, R. C. Scarrow, J. A. Kovacs, *J. Am. Chem. Soc.* **2002**, *124*, 11709–11717.

[74] R. M. Theisen, J. A. Kovacs, *Inorg. Chem.* **2005**, *44*, 1169–1171.

[75] D. T. Sawyer, J. S. Valentine, *Acc. Chem. Res.* **1981**, *14*, 393–400.

[76] J. Shearer, S. B. Fitch, W. Kaminsky, J. Benedict, R. C. Scarrow, J. A. Kovacs, *Proc. Natl. Acad. Sci. USA* **2003**, *100*, 3671–3676.

[77] S. Ozaki, J. Kirose, Y. Kidani, *Inorg. Chem.* **1988**, *27*, 3746–3751.

[78] M. R. Bukowski, K. D. Koehntop, A. Stubna, E. L. Bominaar, J. A. Halfen, E. Münck, W. Nam, L. Que Jr, *Science* **2005**, *310*, 1000–1002.

[79] J.-U. Rohde, J.-H. In, M. H. Lim, W. W. Brennessel, M. R. Bukowski, A. Stubna, E. Munck, W. Nam, L. Que Jr, *Science* **2003**, *299*, 1037–1039.

[80] T. Kitagawa, A. Dey, P. Lugo-Mas, J. Benedict, W. Kaminsky, E. I. Solomon, J. A. Kovacs, **2006**, submitted.

[81] D. L. Harris, G. H. Loew, *J. Am. Chem. Soc.* **1998**, *120*, 8941–8948.

[82] A. Decker, E. I. Solomon, *Curr. Op. Chem. Biol.* **2005**, *9*, 152–163.

[83] E. I. Solomon, A. Decker, N. Lehnert, *Proc. Natl. Acad. Sci. USA* **2003**, *100*, 3589–3594.

[84] S. Ferguson-Miller, G. T. Babcock, *Chem. Rev.* **1996**, *96*, 2889–2907.

[85] N. Lehnert, F. Neese, R. Y. Ho, L. Que Jr, E. I. Solomon, *J. Am. Chem. Soc.* **2002**, *124*, 10810–10822.